

Index theorem with Minimally Doubled Fermions in four space-time dimensions

Abhijeet Kishore^{1,*}, Subhasish Basak^{2,†} and Dipankar Chakrabarti^{1,‡}

¹*Department of Physics, Indian Institute of Technology Kanpur, Kanpur-208016, India and*

²*School of Physical Sciences, National Institute of Science Education and Research,
An OCC of Homi Bhabha National Institute, Jatni-752050, India*

(Dated: February 24, 2026)

We determine the zero eigenmode spectrum of Minimally Doubled Fermions (MDF), namely in Karsten-Wilczek (KW) and Borici-Creutz (BC) formulations on the 4-dimensional space-time lattice. We employ background gauge fields with integer valued topological charges. The Atiyah-Singer index theorem is verified in the presence of two different background gauge fields, namely Smit-Vink [1] and cooled down MILC asqtad ensembles with $N_f = 2 + 1$ dynamical flavors of quarks [2]. Using flavored mass terms [3, 4], we find that the spectral flow of the eigenvalues detects the topology of the background gauge field. With the use of the modified chirality operator, we obtain chiralities of the zero eigenmodes and the fermionic topological charge.

I. INTRODUCTION

Eigenvalue spectra of Dirac operators reflect QCD dynamics such as Bank-Casher relation that relates the zero eigenvalue density, *i.e.*, zero eigenmodes, to the chiral condensate. To obtain and identify zero-eigenmodes, the chiral symmetry needs to be obeyed in the lattice fermion formulation. The two well-known chiral formulations of lattice fermions are overlap [5–9] and domain wall [10–16]. The study of eigenspectra, topology and chiral condensates of these two, along with staggered and Wilson fermions, have been extensively carried out and used to explore the non-perturbative dynamics of QCD.

The continued search for alternative lattice chiral fermions that would be numerically cheaper for QCD simulations led to the proposal of minimally doubled fermions (MDF) with local action that preserves chiral symmetry on the lattice. Two relatively popular implementations of MDF that are mostly explored are those by Karsten-Wilczek (KW) [17, 18] and Borici-Creutz (BC) [19, 20]. A string of investigations on MDF, particularly KW and BC fermions, have been carried out focusing on mixed action spectroscopy [21–25], eigenspectra [26], taste structures [27–30], chiral symmetry breaking [31], and index theorem [3, 4]. Studies on formal aspects include renormalization properties [32–40], phase structure [41–43], anomaly [44], and construction of chiral perturbation theory [30, 45]. Besides, there is a recent attempt to perform dynamical simulation with KW fermions [33].

In this paper, we attempt to investigate the Atiyah-Singer index theorem [46] and the universality of near-zero eigenmodes in sectors with different topological charges [47, 48]. In the presence of background gauge field with an integer valued topological charge, the chiral fermions are expected to satisfy the Atiyah-Singer index theorem. KW and BC fermions are shown to satisfy the index theorem in two dimensions [3, 4, 44, 49, 50]. Here we extend that study to four dimensions. We have constructed four dimensional $SU(3)$ background gauge fields with a fixed topological charge following the prescription of Smit and Vink [1, 51] and observed the flow of eigenvalues as the mass varies. The index of the Hermitian Dirac operator thus obtained from the spectral flow gives us the difference between number of positive and negative chirality zero eigenmodes. For the measurement of the chirality of the zero eigenmodes, we have worked with modified chirality operator and used flavored mass terms [3, 4]. To verify the universality of the zero eigenmodes, we repeated the study with dynamical QCD configurations using the publicly available MILC $N_f = 2 + 1$ asqtad lattices that are subjected to cooling [52] in order to accurately identify various topological charges. This paper is built on and extends our previous work presented in [53].

This paper is organized as follows: following this Introduction, in Sec. II we write down both the KW and BC action in momentum space and point out the doubler species. In Sec. III, we introduce the spectral flow and define the flavored mass. We also describe the generation of background gauge fields with specific topological charge. Subsequently, we study the flow of the eigenvalues against the variation of mass thereby determining the index of the Dirac operator. Following, in Sec. IV, using MILC's dynamical gauge field configurations we employ cooling to identify various topological charge configurations and repeat our spectral flow analysis to reproduce the Index

* akishore@iitk.ac.in

† sbasak@niser.ac.in

‡ dipankar@iitk.ac.in

theorem. Finally, in Sec. V, we conclude with a discussion of our results, along with a summary. We present some results for a different topological charge Q with MILC lattices in Appendix A, and some calculations pertaining to the eigenvalues of the MDF Dirac operator in Appendix B.

II. KARSTEN-WILCZEK AND BORICI-CREUTZ FERMIONS

According to the Nielsen-Ninomiya theorem [54], fermion actions having exact chiral symmetry must have even number of doublers on the lattice. The doublers are extra fermionic species arising because of discretized space-time. The minimum number of doublers on the lattice is two and such fermions are generally referred to as Minimally Doubled Fermions (MDF). The Karsten-Wilczek (KW) [17, 18] and Borici-Creutz (BC) [19, 20] fermions are the two popular members of MDF family. In addition to the naive discretization of the continuum fermion action, both KW and BC contain terms that anticommute with γ_5 , thereby keeping the actions chiral. In Wilson action, a mass-like discretized 4-dimensional Laplacian is added to the naive fermion action that breaks all the chiral symmetries. In contrast, KW fermion multiplies the spatial part of Laplacian by a factor of $i\gamma_4$. It breaks the hypercubic symmetry, but preserves rotational symmetry along the temporal axis, thereby retains chiral symmetry of the lattice action. In 4-dimension, the KW action [38] in the presence of a gauge field $U_\mu(x)$ can be written as

$$S_{\text{KW}} = \sum_x \left[\frac{1}{2} \sum_{\mu=1}^4 \bar{\psi}(x) \gamma_\mu \{ U_\mu(x) \psi(x + \hat{\mu}) - U_\mu^\dagger(x - \hat{\mu}) \psi(x - \hat{\mu}) \} + m \bar{\psi}(x) \psi(x) \right. \\ \left. - \frac{i}{2} \sum_{j=1}^3 \bar{\psi}(x) \gamma_4 \{ U_j(x) \psi(x + \hat{j}) - 2\psi(x) + U_j^\dagger(x - \hat{j}) \psi(x - \hat{j}) \} \right]. \quad (1)$$

The two doubler species become manifest in the Brillouin zone when expressed in momentum space. For simplicity, we consider the free massless KW Dirac operator,

$$D_{\text{KW}}(p) = \sum_{\mu=1}^4 i\gamma_\mu \sin p_\mu + 2i\gamma_4 \sum_{j=1}^3 [\sin(p_j/2)]^2. \quad (2)$$

The poles of the propagator $D_{\text{KW}}^{-1}(p)$ are found to be at $p = (0, 0, 0, 0)$ and $(0, 0, 0, \pi)$ corresponding to the two doublers or tastes, as it is often called.

In BC fermion, the discretized Laplacian is multiplied by a factor of $-i\gamma'_\mu$ which too breaks the hypercubic symmetry, but preserves the rotational symmetry along the axis joining the origin and $(\frac{\pi}{2}, \frac{\pi}{2}, \frac{\pi}{2}, \frac{\pi}{2})$, retaining the chiral symmetry of the lattice action. In 4-dimension, the BC action [38] in the presence of a gauge field $U_\mu(x)$ can be written as

$$S_{\text{BC}} = \sum_x \left[\frac{1}{2} \sum_{\mu=1}^4 \bar{\psi}(x) \gamma_\mu \{ U_\mu(x) \psi(x + \hat{\mu}) - U_\mu^\dagger(x - \hat{\mu}) \psi(x - \hat{\mu}) \} + m \bar{\psi}(x) \psi(x) \right. \\ \left. + \frac{i}{2} \sum_{\mu=1}^4 \bar{\psi}(x) \gamma'_\mu \{ U_\mu(x) \psi(x + \hat{\mu}) - 2\psi(x) + U_\mu^\dagger(x - \hat{\mu}) \psi(x - \hat{\mu}) \} \right], \quad (3)$$

where $\gamma'_\mu = \Gamma - \gamma_\mu$, $\Gamma = (1/2) \sum_{\mu} \gamma_\mu$. Similar to the KW case, we can expose the doublers by working with a free massless theory in momentum space. The corresponding BC Dirac operator is

$$D_{\text{BC}}(p) = \sum_{\mu} i\gamma_\mu \sin p_\mu - 2i \sum_{\mu} \gamma'_\mu [\sin(p_\mu/2)]^2. \quad (4)$$

From $D_{\text{BC}}^{-1}(p)$, it is evident that the poles are at $p = (0, 0, 0, 0)$ and $(\frac{\pi}{2}, \frac{\pi}{2}, \frac{\pi}{2}, \frac{\pi}{2})$. From Eqs. (2, 4) it follows that KW and BC Dirac operators both satisfy γ_5 -hermiticity, $D^\dagger = \gamma_5 D \gamma_5$ and are diagonal in the momentum space.

III. SPECTRAL FLOW AND INDEX

In the continuum, the Atiyah-Singer index theorem relates the difference in the number of negative and positive chirality zero modes of massless Dirac operator to the integer valued topological charge Q in four space-time dimensions [46]

$$\text{index}(D) = n_+ - n_- = Q. \quad (5)$$

The zero modes are eigenstates of the Dirac operator with zero eigenvalues. A large body of studies with Wilson and staggered fermions [1, 55–62] have shown the index theorem to hold on the lattice too. It is also studied for MDF in 2-dimension [3, 4]. An approach to the index theorem on the lattice, away from the continuum, is to consider a hermitian version of the Dirac operator, $H(m) = \gamma_5 (D + m)$, and observe the spectral flow of the eigenvalues of $H(m)$ in a background gauge field. The flow relates the eigenvalues with the topological charge. As the mass varies, the eigenvalue flow shows that those corresponding to the zero-modes cross the origin with slopes \pm , depending on their \pm chiralities, while the non-zero modes do not exhibit any zero-crossing (please refer to Appendix B particularly Eq. (B8)). The index of the Dirac operator is derived from the total number of eigenvalue zero-crossings. The eigenmodes of H can be derived from that of D . If $|\psi\rangle$ is an eigenvector of D with eigenvalue $i\lambda$, then $\gamma_5 |\psi\rangle$ is also an eigenvector of D with eigenvalue $-i\lambda$:

$$D|\psi\rangle = i\lambda|\psi\rangle \implies D(\gamma_5|\psi\rangle) = -i\lambda(\gamma_5|\psi\rangle), \quad \lambda \in \mathbb{R}. \quad (6)$$

Hence, a zero eigenmode $|\psi\rangle$ of D with \pm chirality is also an eigenmode of H with eigenvalue $\pm m$, and therefore crosses the origin with \pm slope as m is varied. For Dirac operators with doubler species having degenerate masses, there is an equal number of positive chirality (n_+) and negative chirality (n_-) states. Thus, the $\text{index}(D)$ in such cases turns out to be zero and the spectral flow obtained for KW and BC fermions shown in the Fig. 1 bears out this fact. The gauge field, used for the flow shown, is generated using Smit-Vink prescription discussed in the following subsection.

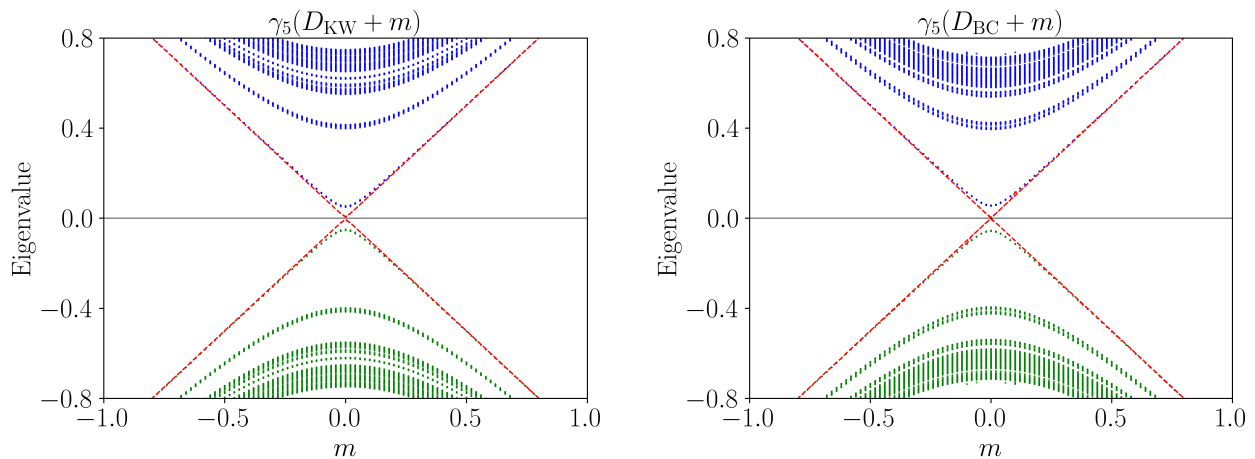


FIG. 1. Spectral flow with respect to degenerate bare masses m for \pm chiral states for both KW and BC fermions under $Q = -2$ and $\delta = 0.05$ background $8^3 \times 8$ Smit-Vink lattice. Eigenvalues in left and right panels correspond to $\gamma_5(D_{KW} + m)$ and $\gamma_5(D_{BC} + m)$, respectively. The color coding is intended to guide the eye.

Connecting the $\text{index}(D)$ with the topological charge seemingly requires careful consideration of the doublers' masses and a better measure of chirality of the zero-modes. We will take up this issue later in the section III C.

A. Gauge configuration with fixed Q

For our study of the index theorem on the lattice with MDF, we generate background gauge configuration with a fixed topological charge Q . Here, we follow the prescription laid out by Smit and Vink in [1, 51] that results in a constant field strength tensor $F_{\mu\nu}(x)$. In terms of $F_{\mu\nu}$, the topological charge on the lattice is defined as

$$\begin{aligned} Q &= \sum_x q(x) = -\frac{1}{32\pi^2} \sum_x \epsilon_{\mu\nu\rho\sigma} \text{Tr}(F_{\mu\nu}F_{\rho\sigma}) \\ &= -\frac{1}{4\pi^2} \sum_x \text{Tr}[F_{12}F_{34} - F_{13}F_{24} + F_{23}F_{14}]. \end{aligned} \quad (7)$$

The lattice sites are $x_\mu \in [0, L_\mu]$ and here we have assumed $L_\mu = L \forall \mu$ where L is the number of sites in each direction, thus $x_\mu = 0, 1, \dots, (L-1)$. The corresponding link variables $U_\mu(x) \in \text{SU}(3)$ are

$$U_1(x) = \exp(-i\omega_1 x_2 \tau_k) \text{ and } U_2(x) = \begin{cases} 1 & \text{for } x_2 = 0, 1, \dots, (L-2) \\ \exp(i\omega_1 L x_1 \tau_k) & \text{for } x_2 = L-1 \end{cases}, \quad (8)$$

$$U_3(x) = \exp(-i\omega_2 x_4 \tau_k) \text{ and } U_4(x) = \begin{cases} 1 & \text{for } x_4 = 0, 1, \dots, (L-2) \\ \exp(i\omega_2 L x_3 \tau_k) & \text{for } x_4 = L-1 \end{cases}, \quad (9)$$

where τ_k is any one of the Gell-Mann matrices with $k = 1, 2, \dots, 7$. The $\omega_{1,2}$ are constant field strength given by

$$\omega_{1,2} = \frac{2\pi n_{1,2}}{L^2} \text{ where } n_{1,2} \in \mathbb{Z}. \quad (10)$$

The gauge links thus defined, the elementary plaquettes become constant,

$$\begin{aligned} U_{\mu\nu}(x) &= U_\mu(x)U_\nu(x + \hat{\mu})U_\mu^\dagger(x + \hat{\nu})U_\nu^\dagger(x), \\ U_{12}(x) &= \exp(i\omega_1 \tau_k), \quad U_{34} = \exp(i\omega_2 \tau_k) \text{ and the rest } U_{\mu\nu}(x) = 1. \end{aligned} \quad (11)$$

The field tensor $F_{\mu\nu}$ extracted from the above elementary plaquette $U_{\mu\nu}$ in (11) yields,

$$F_{\mu\nu}(x) = \frac{1}{2i} [U_{\mu\nu}(x) - U_{\mu\nu}^\dagger(x)]_{\text{AH}} \quad (12)$$

$$\Rightarrow F_{12} = \tau_k \sin(\omega_1), \quad F_{34} = \tau_k \sin(\omega_2) \text{ and the rest } F_{\mu\nu} = 0. \quad (13)$$

The subscript AH implies traceless anti-hermitian projection. From the definition in (7), the topological charge is obtained to be,

$$Q = -\frac{1}{4\pi^2} \sum_x \text{Tr} [F_{12} F_{34}] = -\frac{2L^4}{4\pi^2} \sin\left(\frac{2\pi n_1}{L^2}\right) \sin\left(\frac{2\pi n_2}{L^2}\right) \approx -2n_1 n_2, \quad (14)$$

where the last result is for (moderately) large L . For τ_8 , *i.e.* $k = 8$, the above derivation does not hold, but in the large volume limit, it too gives us $-2n_1 n_2$ as topological charge.

The gauge fields $U_\mu(x)$ thus generated correspond to a given Q depending on n_1, n_2 . These fields are considered smooth in the sense that they are not elements of a Markov chain. Such a smooth configuration may not always give well-separated sign flips in the flow of eigenvalues of the Dirac operator. Hence ‘roughening’ the $U_\mu(x)$ by keeping Q approximately invariant has been suggested [1, 51]. The idea is to generate some θ_μ^k from uniformly distributed random numbers $\in [-\delta\pi, +\delta\pi]$, where $\delta \ll 1$, in order to roughen the links $U_\mu(x)$ in Eqs. (8, 9),

$$U_\mu^\delta(x) = \exp\left(i \sum_k \theta_\mu^k \tau_k\right) \rightarrow \tilde{U}_\mu(x) = U_\mu^\delta(x) U_\mu(x), \quad (15)$$

where \tilde{U}_μ are the roughened gauge fields. In all subsequent calculations with Smit-Vink gauge fields, presented in the tables and plots in this section, we use such rough gauge fields $\tilde{U}_\mu(x)$ generated on $8^3 \times 8$ lattice with $Q = -2$ and $\delta = 0.05$.

B. Determination of the near-zero eigenvalues

The computation of zero or near-zero eigenvalues is carried out by using the Kalkreuter-Simma (KS) algorithm [63]. It provides both eigenvectors and eigenvalues for any hermitian matrix and not just only for positive definite matrices. We implement the algorithm by suitably modifying the relevant subroutines in the publicly available MILC code [64]. The hermitian version of the Dirac MDF operator is

$$H(m) = \gamma_5(D + m) \Rightarrow H^2(m) = (D^\dagger + m)(D + m), \quad (16)$$

where H, D are either of KW or BC. The eigenvalues of $H(m)$ appear with both signs; therefore, obtaining the near-zero eigenvalues by direct computation is not practical even for a modest 4-dimensional lattice volume. This problem can be sidestepped by using $H^2(m)$ to solve the eigenvalue equation $H^2(m)|\psi_j\rangle = \lambda_j|\psi_j\rangle$, where the lowest

eigenvalues are always non-negative and close to zero. However, in general, neither $|\psi_j\rangle$ nor $\pm\sqrt{\lambda_j}$ are necessarily the eigenvectors or eigenvalues of $H(m)$. Nevertheless, to a good approximation, the eigenvectors of $H(m)$, and hence the near-zero eigenvalues, can be obtained by following the Rayleigh-Ritz procedure [65]. Following this procedure, once a desired number (typically a few hundred) of the lowest eigenvalues and their corresponding eigenvectors, say $|\psi'\rangle$, are obtained, a reduced matrix \mathcal{M} of $H(m)$ can be constructed, and the resulting eigenvalue problem is solved,

$$\mathcal{M}_{xy} = \langle \psi'_x | H(m) | \psi'_y \rangle \rightarrow \mathcal{M} |\chi_x\rangle = \mu_x |\chi_x\rangle. \quad (17)$$

An approximate eigenvector $|\phi\rangle$ of $H(m)$ can be calculated as

$$|\phi_k\rangle = \sum_x \chi_k^x |\psi'_x\rangle, \quad (18)$$

where χ_k^x is the x -th component of k -th normalized eigenvector of \mathcal{M} . This kind of rotation is a feature in the KS algorithm [63], which is called intermediate diagonalization, and is used to improve previously computed eigenvectors of a matrix. The eigenvalue equation for $H(m)$, for lowest lying eigenvalue, in the subspace of $H^2(m)$ is now

$$H(m)|\phi_k\rangle \approx \mu_k |\phi_k\rangle, \quad (19)$$

$$\text{with residue } r_k = \|(H(m) - \mu_k)|\phi_k\rangle\| \approx 0. \quad (20)$$

Eigenvalue of H_{KW}^2	Eigenvalue of H_{KW}	r_k	Eigenvalue of H_{BC}^2	Eigenvalue of H_{BC}	r_k
2.462×10^{-5}	-4.962×10^{-3}	5×10^{-6}	4.041×10^{-7}	-6.356×10^{-4}	6×10^{-6}
2.462×10^{-5}	4.962×10^{-3}	5×10^{-6}	4.041×10^{-7}	6.356×10^{-4}	6×10^{-6}
4.808×10^{-5}	-6.934×10^{-3}	6×10^{-6}	1.820×10^{-5}	-4.266×10^{-3}	5×10^{-6}
4.808×10^{-5}	6.934×10^{-3}	6×10^{-6}	1.820×10^{-5}	4.266×10^{-3}	5×10^{-6}
2.420×10^{-3}	-4.919×10^{-2}	7×10^{-6}	2.955×10^{-3}	-5.436×10^{-2}	4×10^{-6}
2.420×10^{-3}	4.919×10^{-2}	7×10^{-6}	2.955×10^{-3}	5.436×10^{-2}	4×10^{-6}
2.468×10^{-3}	-4.968×10^{-2}	7×10^{-6}	3.038×10^{-3}	-5.512×10^{-2}	5×10^{-6}
2.468×10^{-3}	4.968×10^{-2}	7×10^{-6}	3.038×10^{-3}	5.512×10^{-2}	5×10^{-6}
2.905×10^{-3}	-5.389×10^{-2}	6×10^{-6}	3.186×10^{-3}	-5.644×10^{-2}	6×10^{-6}

TABLE I. For $m = 0$, we tabulate eigenvalues of H^2 and H with residues r_k as in Eq. (20) for $Q = -2$ and $\delta = 0.05$ background $8^3 \times 8$ Smit-Vink lattice.

Eigenvalue of H_{KW}^2	Eigenvalue of H_{KW}	r_k	Eigenvalue of H_{BC}^2	Eigenvalue of H_{BC}	r_k
1.442×10^{-2}	-1.201×10^{-1}	5×10^{-6}	1.440×10^{-2}	-1.200×10^{-1}	6×10^{-6}
1.442×10^{-2}	1.201×10^{-1}	5×10^{-6}	1.440×10^{-2}	1.200×10^{-1}	6×10^{-6}
1.445×10^{-2}	-1.202×10^{-1}	6×10^{-6}	1.442×10^{-2}	-1.201×10^{-1}	4×10^{-6}
1.445×10^{-2}	1.202×10^{-1}	6×10^{-6}	1.442×10^{-2}	1.201×10^{-1}	5×10^{-6}
1.682×10^{-2}	-1.297×10^{-1}	7×10^{-6}	1.735×10^{-2}	-1.317×10^{-1}	3×10^{-6}
1.682×10^{-2}	1.297×10^{-1}	7×10^{-6}	1.735×10^{-2}	1.317×10^{-1}	5×10^{-6}
1.687×10^{-2}	-1.299×10^{-1}	6×10^{-6}	1.744×10^{-2}	-1.321×10^{-1}	3×10^{-6}
1.687×10^{-2}	1.299×10^{-1}	7×10^{-6}	1.744×10^{-2}	1.321×10^{-1}	3×10^{-6}
1.730×10^{-2}	-1.315×10^{-1}	6×10^{-6}	1.759×10^{-2}	-1.326×10^{-1}	4×10^{-6}

TABLE II. Same as Table. I but for some small, non-zero mass $m = 0.12$.

The $|\phi_k\rangle$ is the approximate eigenvector with approximate eigenvalue μ_k , *i.e.*, $r_k \approx 0$. For ‘good’ eigenvalues and hence ‘good’ eigenvectors, r_k should be small.¹ In Table I and II we present a representative sample of residues for $m = 0$ and $m = 0.12$, respectively. Eigenvalues of H^2 are calculated with a numerical tolerance of $\mathcal{O}(10^{-6})$.

¹ While using the Rayleigh-Ritz procedure [53], we encounter some spurious eigenvalues of H at the top end of the near-zero eigenmodes. These originate from errors in determining the corresponding eigenvalues and eigenvectors of H^2 . We discard a few such high-lying eigenmodes, thereby eliminating the spurious eigenmodes and improving the accuracy of the eigenmodes of H .

C. Flavored mass and Index theorem

In the Fig. 1, we were unable to detect the index using spectral flow, despite using gauge fields with a specific non-zero integer value of Q . For MDF with degenerate doublers, the index gets cancelled between the pairs and hence the flow of eigenvalue with such mass term $m(1 \otimes 1)$ does not result in net crossings at $m \approx 0$. The degeneracy in masses for \pm chiral states is made apparent from the plot of the complex eigenvalues (Eq. (6)) of the operator $(D + m(1 \otimes 1))$ in Fig. 2.

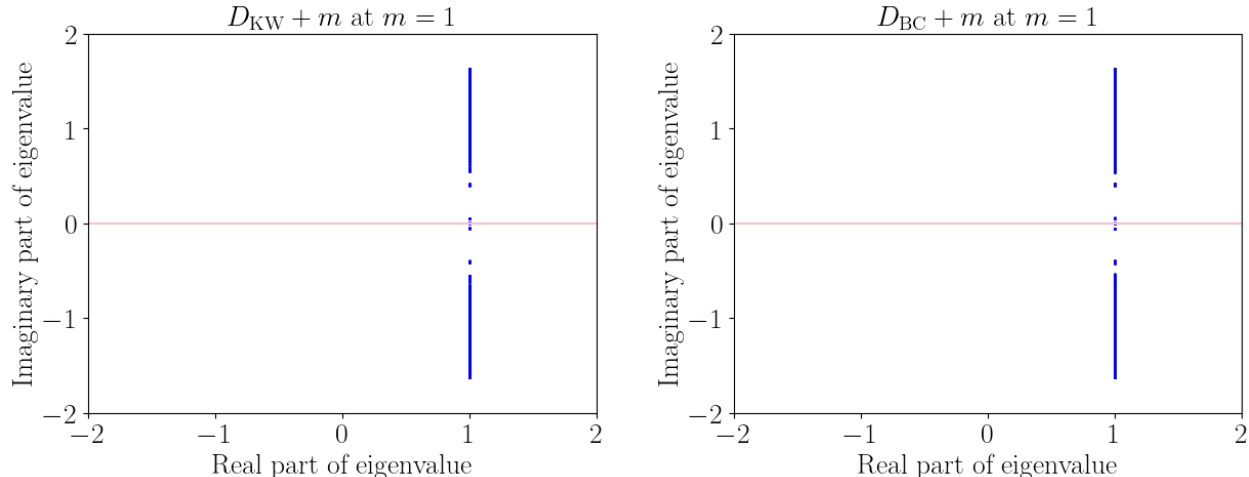


FIG. 2. Complex eigenvalue plots of KW and BC fermions for $Q = -2$ and $\delta = 0.05$ background $8^3 \times 8$ Smit-Vink lattice with mass parameter $m = 1$ for 5000 eigenvalues. The left and right panel correspond to $(D_{\text{KW}} + m)$ and $(D_{\text{BC}} + m)$.

The problem of degeneracy in real eigenvalues can be resolved by lifting the degeneracy of the masses of \pm chiral states by introducing a doubler or taste dependent so-called ‘flavored mass term’, $mC_{\text{flav}} \otimes 1$ [3, 4]

$$C_{\text{flav}}^{\text{KW}} = C_{\text{sym}} \quad \text{and} \quad C_{\text{flav}}^{\text{BC}} = 2C_{\text{sym}} - 1, \quad (21)$$

$$\text{where} \quad C_{\text{sym}} = \frac{1}{4!} \sum_{\text{perm}} C_1 C_2 C_3 C_4, \quad (22)$$

$$\text{and} \quad C_\mu(x, y) |\psi(y)\rangle = \frac{1}{2} [U_\mu(x) \delta_{x+\hat{\mu}, y} + U_\mu^\dagger(x - \hat{\mu}) \delta_{x-\hat{\mu}, y}] |\psi(y)\rangle. \quad (23)$$

The eigenvalues of the flavored MDF operators $(D + mC_{\text{flav}} \otimes 1)$ are shown in Fig. 3 for free theory. The separation of the zero eigenvalues along the real axis at $\pm m$ for KW, and appropriately shifted for BC, shows removal of the degeneracy discussed above. When the background gauge field with a particular topological charge is turned on, we observe similar splittings of the low-lying states as shown in Fig. 4.

Next, we calculate the eigenvalues of $(D + mC_{\text{flav}})$ with Smit-Vink gauge field. Since $(D + mC_{\text{flav}})$ is a non-hermitian and non-normal operator, its eigenvalues are complex, and left- and right-eigenvectors are not related by the adjoint operation [66]. To obtain its eigenvalues, we construct a reduced matrix for $(D + mC_{\text{flav}})$ using the eigenvectors of hermitian $(D^\dagger + mC_{\text{flav}})(D + mC_{\text{flav}})$, and compute the eigenvalues of this reduced matrix. We found many ‘spurious’ eigenvalues in this set but as the size of the reduced matrix is increased, these spurious eigenvalues disappear.

When the simple mass-term is replaced by mC_{flav} mass for both KW and BC fermions, the spectral flow in Fig. 5 exhibits the exact number of crossings as required by the expression in Eq. (26). We have two lines crossing near $m = 0$ with negative slopes and each being two-fold degenerate, for both KW and BC fermions. The flow shown in Fig. 5 corresponds to the eigenvalues of the associated Hermitian MDF operators

$$\mathcal{H}_{\text{KW}}(m) = \gamma_5 (D_{\text{KW}} + mC_{\text{sym}} \otimes 1), \quad (24)$$

$$\mathcal{H}_{\text{BC}}(m) = \gamma_5 (D_{\text{BC}} + m(2C_{\text{sym}} - 1) \otimes 1). \quad (25)$$

In this case, the index theorem acquires an additional factor of 2 arising from two non-degenerate masses of the doubler species, depending on their \pm chirality [3]

$$\text{index}(D) = 2Q. \quad (26)$$

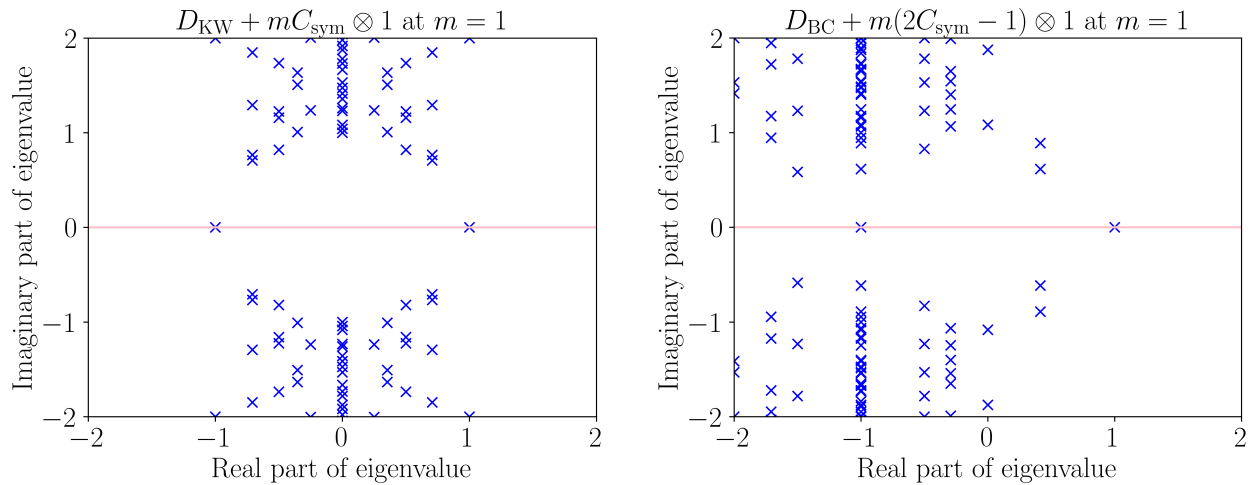


FIG. 3. Complex eigenvalue plots of KW and BC fermions for free theory on $8^3 \times 8$ lattice with mass parameter $m = 1$. The left and right panel correspond to $(D_{\text{KW}} + mC_{\text{sym}} \otimes 1)$ and $(D_{\text{BC}} + m(2C_{\text{sym}} - 1) \otimes 1)$ operators, respectively.

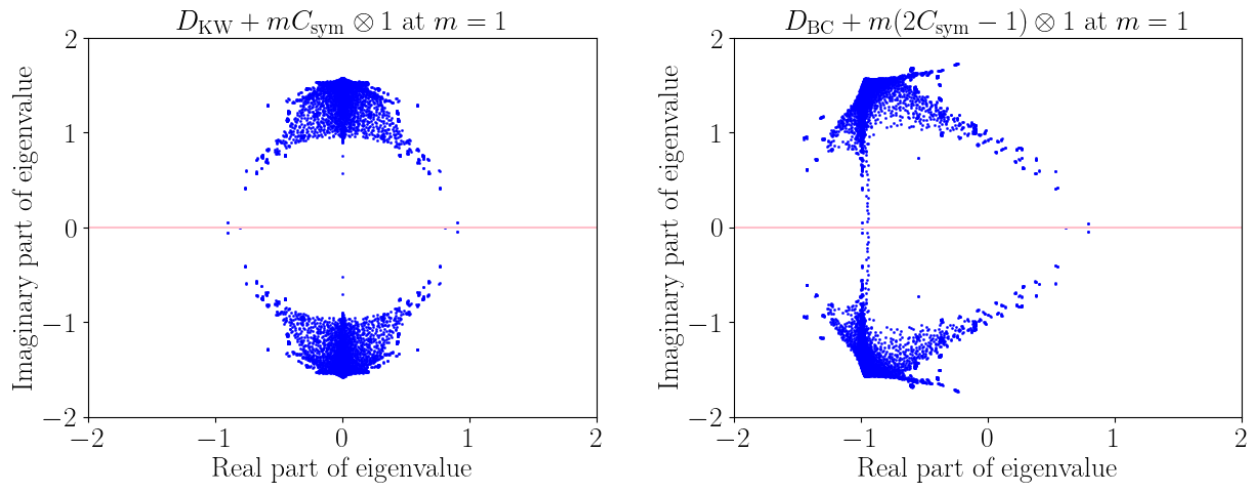


FIG. 4. Same plot as Fig. 3 but with $Q = -2$ and $\delta = 0.05$ background $8^3 \times 8$ Smit-Vink lattice.

To obtain the near-zero modes of \mathcal{H} , we proceed as before to first find the lowest-lying eigenvalues of the operator \mathcal{H}^2 . Followed by constructing a reduced matrix \mathcal{M} as in Eq. (17) and its eigenstates, whose linear combination serves as basis states (rotational basis) of \mathcal{H} . The result is tabulated below in Table. III.

To determine the chiral states of the eigenvectors $|\psi\rangle$ of the MDF operator D in Eq. (6), we observe that both $|\psi\rangle$ and $\gamma_5|\psi\rangle$ are eigenvectors with eigenvalues $\pm i\lambda$. For $\lambda = 0$, the corresponding eigenvector can also be chosen as a simultaneous eigenvector of γ_5 (see Eq. (B4)). In general, when we calculate the eigenvalues of D , then we do not impose the condition on eigenvectors of D with zero eigenvalues to be simultaneous eigenvectors of γ_5 . Consequently, arbitrary linear combinations of these chiral states are also eigenvectors of D with $\lambda = 0$. In such cases, we get $\langle\psi|\gamma_5|\psi\rangle \approx 0$. A brief discussion on this aspect is provided in Appendix B (see Eq. (B11)). Our numerical results yield $\langle\gamma_5\rangle \approx 0$, implying that the zero-mode eigenvectors in our setup are not simultaneous eigenvectors of D and γ_5 . Therefore, we cannot determine the chiralities of the zero eigenmodes with γ_5 operator. Hence, modified chirality operators \mathcal{X} are proposed [4]

$$\mathcal{X}_{\text{KW}} = C_{\text{sym}} \otimes \gamma_5 \quad \text{and} \quad \mathcal{X}_{\text{BC}} = (2C_{\text{sym}} - 1) \otimes \gamma_5. \quad (27)$$

In Table IV, we list the lowest-lying eigenvalues and their corresponding chiralities, computed using the eigenvectors of $H(m = 0)$ [12] rather than D . This choice is motivated by the poor residues obtained when attempting to construct the eigenvectors of D from $H^2(m = 0)$ for various lattice sizes. Using $H(m = 0)$ is justified for two reasons: (i) for zero-modes ($\lambda = 0$), the eigenvectors of D and $H(m = 0)$ are identical (see Eq. (B10)), and (ii) for $\lambda \neq 0$, the

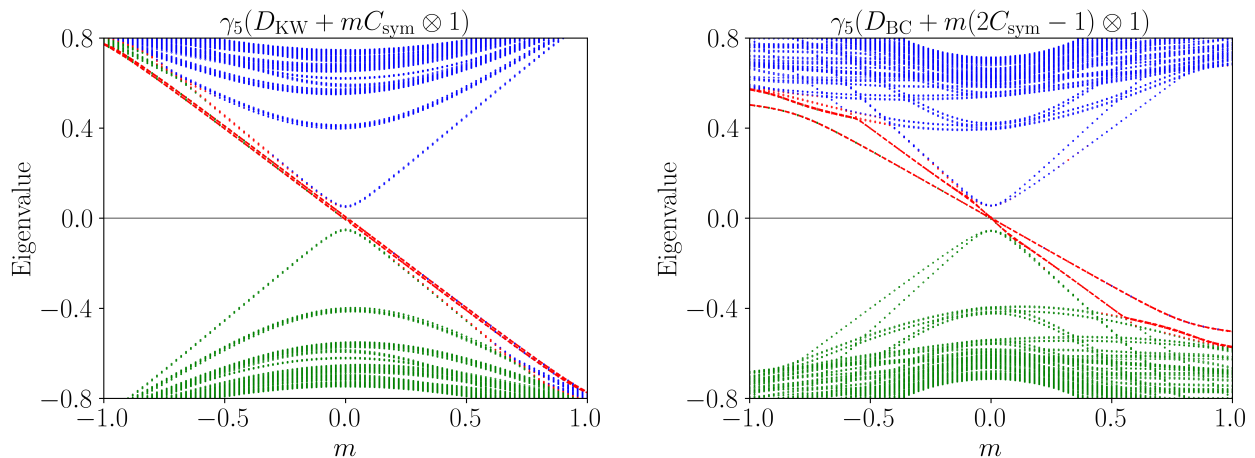


FIG. 5. Spectral flow of the eigenvalues of \mathcal{H} with respect to m for $Q = -2$ and $\delta = 0.05$ background Smit-Vink lattice. Four nearly overlapping lines (red in color) cross the zero eigenvalue line at $m = 0$. The color coding is intended to guide the eye.

Eigenvalue of $\mathcal{H}_{\text{KW}}^2$	Eigenvalue of \mathcal{H}_{KW}	r_k	Eigenvalue of $\mathcal{H}_{\text{BC}}^2$	Eigenvalue of \mathcal{H}_{BC}	r_k
8.055×10^{-3}	-8.975×10^{-2}	5×10^{-7}	5.120×10^{-3}	-7.155×10^{-2}	1×10^{-6}
8.435×10^{-3}	-9.184×10^{-2}	5×10^{-7}	5.229×10^{-3}	-7.231×10^{-2}	1×10^{-6}
1.034×10^{-2}	-1.017×10^{-1}	4×10^{-7}	1.102×10^{-2}	-1.050×10^{-1}	1×10^{-6}
1.065×10^{-2}	-1.032×10^{-1}	4×10^{-7}	1.202×10^{-2}	-1.096×10^{-1}	1×10^{-6}
1.380×10^{-2}	1.175×10^{-1}	4×10^{-7}	1.202×10^{-2}	1.096×10^{-1}	1×10^{-6}
1.388×10^{-2}	1.178×10^{-1}	6×10^{-7}	1.210×10^{-2}	1.100×10^{-1}	2×10^{-6}
1.388×10^{-2}	-1.178×10^{-1}	5×10^{-7}	1.440×10^{-2}	-1.200×10^{-1}	1×10^{-6}
1.404×10^{-2}	-1.185×10^{-1}	5×10^{-7}	1.561×10^{-2}	-1.250×10^{-1}	1×10^{-6}
1.497×10^{-2}	1.223×10^{-1}	3×10^{-7}	1.732×10^{-2}	1.316×10^{-1}	1×10^{-6}

TABLE III. For $m = 0.12$, we tabulate eigenvalues of \mathcal{H}^2 and \mathcal{H} with residues r_k for $Q = -2$ and $\delta = 0.05$ background $8^3 \times 8$ Smit-Vink lattice.

expectation value $\langle \psi | \gamma_5 | \psi \rangle$ vanishes for either operator (see Eqs. (B6, B9)). While $\langle \gamma_5 \rangle \approx 0$ throughout, the modified chirality operator \mathcal{X} correctly identifies the chiralities for zero eigenmodes for any Q , yielding an index of $2Q$, in agreement with the index theorem. Notably, since C_{flav} does not commute with D in presence of gauge fields [3], the modified chirality \mathcal{X} can never attain exact ± 1 for chiral states.

Eigenvalue of $H_{\text{KW}}(m=0)$	$\langle \psi_i \mathcal{X}_{\text{KW}} \psi_i \rangle$	Eigenvalue of $H_{\text{BC}}(m=0)$	$\langle \psi_i \mathcal{X}_{\text{BC}} \psi_i \rangle$
-4.962×10^{-3}	-8.037×10^{-1}	-6.356×10^{-4}	-7.935×10^{-1}
4.962×10^{-3}	-8.037×10^{-1}	6.356×10^{-4}	-7.935×10^{-1}
-6.934×10^{-3}	-7.995×10^{-1}	-4.266×10^{-3}	-7.771×10^{-1}
6.934×10^{-3}	-7.995×10^{-1}	4.266×10^{-3}	-7.771×10^{-1}
-4.919×10^{-2}	-9.096×10^{-4}	-5.436×10^{-2}	-1.892×10^{-3}
4.919×10^{-2}	-9.096×10^{-4}	5.436×10^{-2}	-1.892×10^{-3}
-4.968×10^{-2}	-6.392×10^{-3}	-5.512×10^{-2}	-1.106×10^{-3}

TABLE IV. Eigenvalues and modified chirality \mathcal{X} using eigenvectors of $H(m=0)$ for $Q = -2$ and $\delta = 0.05$ background $8^3 \times 8$ Smit-Vink lattice.

In Fig. 6, we plotted the expectation of modified chirality operator \mathcal{X} against various eigenmodes, among which we found 4 of them with chirality -1 (approximately). The imaginary part of the eigenvalues of D are shown in Fig. 7. We observe that non-zero eigenvalues of D form clusters of doublets because of the doubler species.

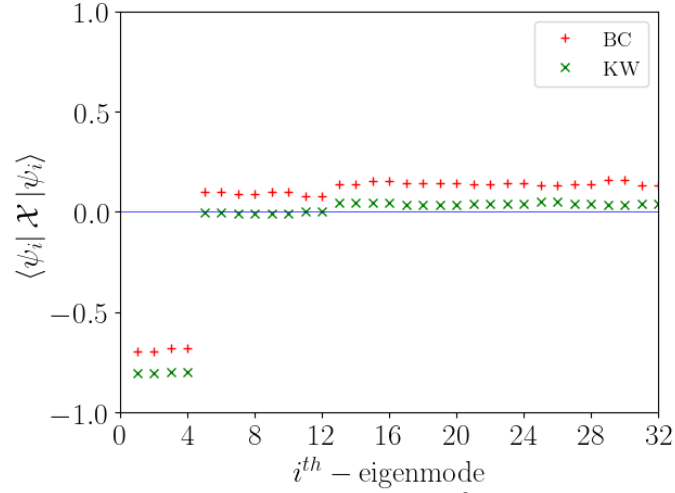


FIG. 6. The modified chirality \mathcal{X} for $Q = -2$ and $\delta = 0.05$ background $8^3 \times 8$ Smit-Vink lattice. For clarity, $\langle \mathcal{X}_{\text{BC}} \rangle$ is shifted by +0.1.

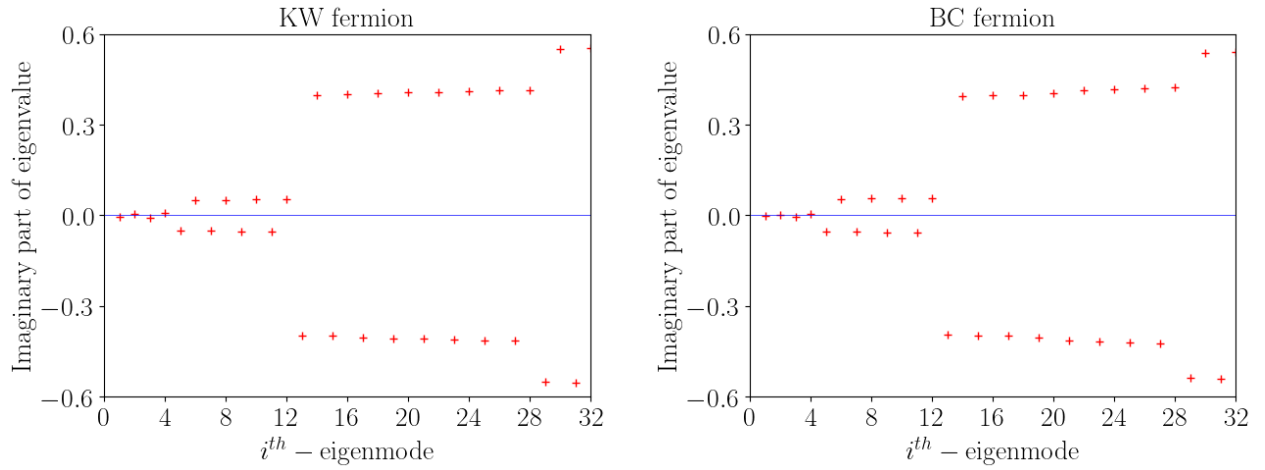


FIG. 7. Non-zero eigenvalues form clusters of doublets, while the number of zero eigenvalues depends on the background topology. The results are for $Q = -2$ and $\delta = 0.05$ background $8^3 \times 8$ Smit-Vink lattice.

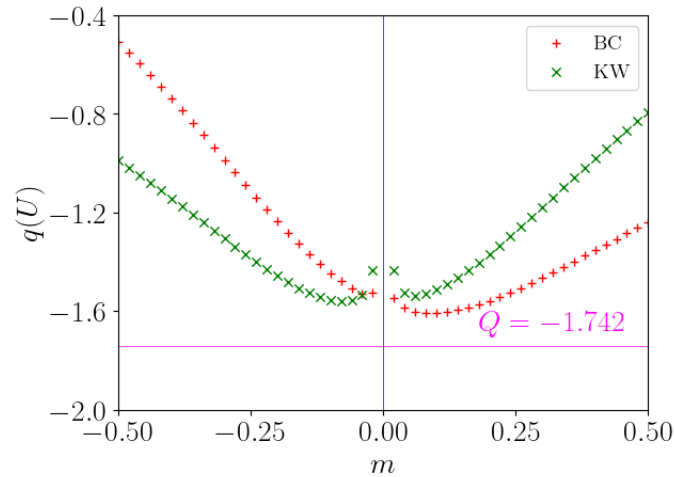


FIG. 8. Variation of fermionic topological charge with m for $Q = -2$ and $\delta = 0.05$ background $8^3 \times 8$ Smit-Vink Lattice. Q is measured to be -1.742 .

An alternative way to verify the index theorem is using the fermionic topological charge [1, 4, 67, 68]. In the continuum on a background field A_μ with topological charge $Q \in \mathbb{Z}$, it is given by

$$q(A) = \lim_{m \rightarrow 0} m \text{Tr} [\gamma_5 (D + m)^{-1}]. \quad (28)$$

For MDF in the presence of background gauge fields U_μ , this expression becomes

$$q(U) = \lim_{m \rightarrow 0} \frac{m}{2} \text{Tr} [(C_{\text{flav}} \otimes \gamma_5) (D + m)^{-1}]. \quad (29)$$

In Fig. 8, if we neglect a small pole like structure near $m = 0$ then we can read the $q(U)$ to be approximately -1.6 . It deviates slightly from the $Q = -1.742$ measured using Eq. (14) with the improved field strength tensor $F_{\mu\nu}^I$ given in Eq. (34). This may be attributed to the roughening of $Q = -2$ Smit-Vink field, which is performed in a way that approximately preserves the original Q . We observe that in Fig. 8 an apparent divergence of $q(U)$ appears around $m = 0$, which vanishes for larger lattice volume. Its appearance could be due to our use of a rather small lattice volume of $8^3 \times 8$.

IV. INDEX THEOREM ON DYNAMICAL QCD LATTICES

In the previous section, we showed that the index theorem holds for MDF in 4-dimension on Smit-Vink type lattices. In this section, we attempt to explore how the theorem holds up on QCD lattices. For this purpose, we use MILC asqtad $N_f = 2 + 1$ lattices [2]. We choose coarse $16^3 \times 48$ lattices with $10/g_0^2 = 6.572$ and $a \approx 0.15$ fm followed by smoothing steps, which is called ‘‘cooling’’. Smoothing steps have been central to the study of topology and instantons in QCD [52], as the topological charge of gauge fields is highly sensitive to these procedures. In particular, smoothing/cooling significantly improves the reliability of identifying topological charges. This is essential to accurately establish the universality of the expression in Eq. (26). For this work, we utilize the cooling algorithm described in Ref. [52]; however, unlike that approach, we do not perform any smearing steps. To proceed further, we reproduce some of its expressions that are relevant for our case.

The cooling algorithm essentially constructs improved staples to define an ‘‘improved’’ topological charge. The improved staples $\Sigma_{\mu\nu}^I(x)$ consist of a linear combination of square and rectangular staples in $\mu - \nu$ plane,

$$\Sigma_{\mu\nu}^I(x) = \frac{5}{3} \Sigma_{\mu\nu}(x) + \frac{1}{12u_0^2} \Sigma_{\mu\nu}^R(x), \quad (30)$$

$$\text{where } \Sigma_{\mu\nu}(x) = U_\nu(x + \hat{\mu}) U_\mu^\dagger(x + \hat{\nu}) U_\nu^\dagger(x) + U_\nu^\dagger(x + \hat{\mu} - \hat{\nu}) U_\mu^\dagger(x - \hat{\nu}) U_\nu(x - \hat{\nu}), \quad (31)$$

$$\begin{aligned} \text{and } \Sigma_{\mu\nu}^R(x) = & U_\mu(x + \hat{\mu}) U_\nu(x + 2\hat{\mu}) U_\mu^\dagger(x + \hat{\mu} + \hat{\nu}) U_\mu^\dagger(x + \hat{\nu}) U_\nu^\dagger(x) + \\ & U_\nu(x + \hat{\mu}) U_\nu(x + \hat{\mu} + \hat{\nu}) U_\mu^\dagger(x + 2\hat{\nu}) U_\nu^\dagger(x + \hat{\nu}) U_\nu^\dagger(x) + \\ & U_\nu(x + \hat{\mu}) U_\mu^\dagger(x + \hat{\nu}) U_\mu^\dagger(x - \hat{\mu} + \hat{\nu}) U_\nu^\dagger(x - \hat{\mu}) U_\mu(x - \hat{\mu}) + \\ & U_\nu^\dagger(x + \hat{\mu} - \hat{\nu}) U_\mu^\dagger(x - \hat{\nu}) U_\mu^\dagger(x - \hat{\mu} - \hat{\nu}) U_\nu(x - \hat{\mu} - \hat{\nu}) U_\mu(x - \hat{\mu}) + \\ & U_\nu^\dagger(x + \hat{\mu} - \hat{\nu}) U_\nu^\dagger(x + \hat{\mu} - 2\hat{\nu}) U_\mu^\dagger(x - 2\hat{\nu}) U_\nu(x - 2\hat{\nu}) U_\nu(x - \hat{\nu}) + \\ & U_\mu(x + \hat{\mu}) U_\nu^\dagger(x + 2\hat{\mu} - \hat{\nu}) U_\mu^\dagger(x + \hat{\mu} - \hat{\nu}) U_\mu^\dagger(x - \hat{\nu}) U_\nu(x - \hat{\nu}), \end{aligned} \quad (32)$$

where u_0 is the tadpole factor that gets updated after each iteration through the lattice. The action of cooling results in replacing the original links $U_\mu(x)$ by the links that maximizes

$$\max \text{Re Tr} \left(U_\mu(x) \sum_{\substack{\nu \\ \nu \neq \mu}} \Sigma_{\mu\nu}^I(x) \right). \quad (33)$$

The improved links define the $\mathcal{O}(a^2)$ improved field strength tensor $F_{\mu\nu}^I(x)$ which is used for topological charge to ensure (nearly) integer value of Q defined in Eq. (7).

$$F_{\mu\nu}^I(x) = \frac{5}{3} \Omega_{\mu\nu}^{(1,1)}(x) - \frac{1}{3} \Omega_{\mu\nu}^{(1,2)}(x), \quad (34)$$

$$\text{where } \Omega_{\mu\nu}^{(1,1)}(x) = \frac{1}{2i} (C_{\mu\nu}^{(1,1)}(x) - C_{\mu\nu}^{(1,1)\dagger})_{\text{AH}}, \quad (35)$$

$$\text{and } \Omega_{\mu\nu}^{(1,2)}(x) = \frac{1}{2i} (C_{\mu\nu}^{(1,2)}(x) - C_{\mu\nu}^{(1,2)\dagger})_{\text{AH}}. \quad (36)$$

The subscript AH implies traceless anti-hermitian projection. The $C_{\mu\nu}$'s are clover leaf arrangements of 1×1 square and 2×1 rectangular plaquettes,

$$P_{\mu\nu}^{(1 \times 1)}(x) = U_\mu(x) U_\nu(x + \hat{\mu}) U_\mu^\dagger(x + \hat{\nu}) U_\nu^\dagger(x), \quad (37)$$

$$P_{\mu\nu}^{(1 \times 2)}(x) = U_\mu(x) U_\nu(x + \hat{\mu}) U_\nu(x + \hat{\mu} + \hat{\nu}) U_\mu^\dagger(x + 2\hat{\nu}) U_\nu^\dagger(x + \hat{\nu}) U_\nu^\dagger(x), \quad (38)$$

$$P_{\mu\nu}^{(2 \times 1)}(x) = U_\mu(x) U_\mu(x + \hat{\mu}) U_\nu(x + 2\hat{\mu}) U_\mu^\dagger(x + \hat{\mu} + \hat{\nu}) U_\mu^\dagger(x + \hat{\nu}) U_\nu^\dagger(x), \quad (39)$$

$$C_{\mu\nu}^{(1,1)}(x) = \frac{1}{4} (P_{\mu\nu}^{(1 \times 1)}(x) + P_{-\mu\nu}^{(1 \times 1)}(x) + P_{\mu-\nu}^{(1 \times 1)}(x) + P_{-\mu-\nu}^{(1 \times 1)}(x)), \quad (40)$$

$$C_{\mu\nu}^{(1,2)}(x) = \frac{1}{8} (P_{\mu\nu}^{(2 \times 1)}(x) + P_{-\mu\nu}^{(2 \times 1)}(x) + P_{\mu-\nu}^{(2 \times 1)}(x) + P_{-\mu-\nu}^{(2 \times 1)}(x) \\ + P_{\mu\nu}^{(1 \times 2)}(x) + P_{-\mu\nu}^{(1 \times 2)}(x) + P_{\mu-\nu}^{(1 \times 2)}(x) + P_{-\mu-\nu}^{(1 \times 2)}(x)). \quad (41)$$

The topological charge Q , now defined using $F_{\mu\nu}^I$, is plotted as a function of the number of cooling sweeps n_{sweep} in Fig. 9. Cooling reduces the fluctuations in Q and leads to stable plateaus, typically after 60 sweeps, at near-integer values. This evolution of Q is found consistent with Ref. [52].

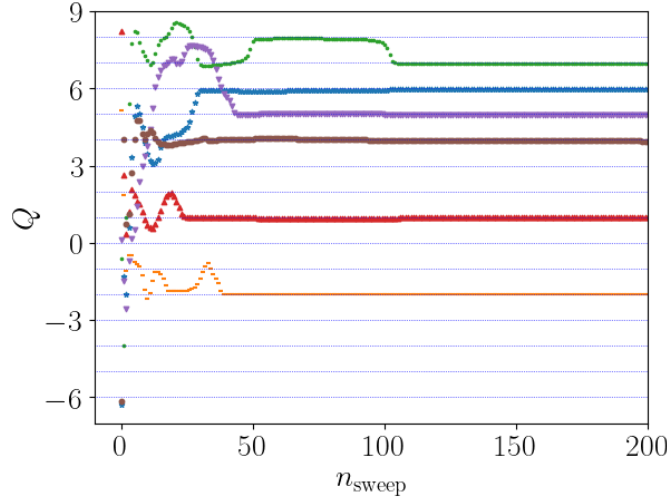


FIG. 9. Variation of Q as a function of cooling sweeps n_{sweep} on six configurations of MILC $16^3 \times 48$ lattice.

To remain consistent with the previous case of $Q = -2$ for Smit-Vink lattice, we select the MILC configuration with $Q = -1.997$, which is closest to -2 , for the spectral flow and subsequent analysis. Before analyzing the spectral flow, we cross-check the Q value for the chosen configuration by calculating the fermionic topological charge q , as defined in Eq. (29). As in the previous section, we examine the mass dependence of q and verify whether $q(m \rightarrow 0) \approx Q$. This behaviour is illustrated in Fig. 10 for $Q \approx -2$. The same procedure is applied to a few other configurations with different Q , for example see Fig. 15 for $Q \approx -3$.

For the MILC configuration with $Q \approx -2$, we present in Fig. 11 the spectral flow of the near-zero eigenvalues of the hermitian MDF Dirac operator with a flavor-dependent mass term. The net number of eigenvalue crossings is consistent with index $= -4 \approx 2Q$.

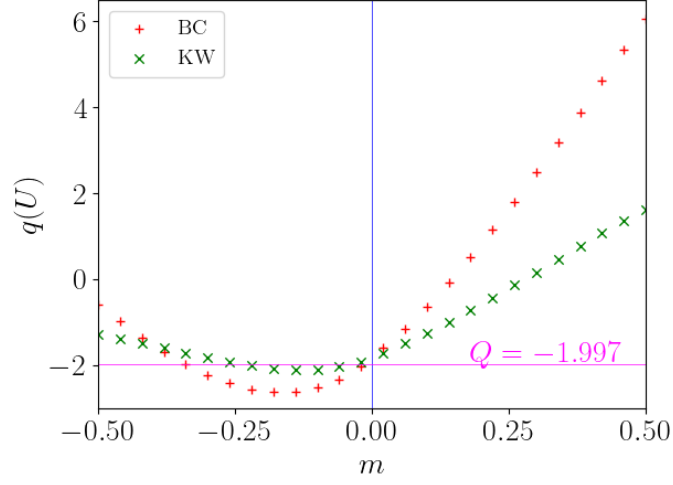


FIG. 10. Variation of fermionic topological charge with m for $Q = -1.997$ background $16^3 \times 48$ MILC lattice.

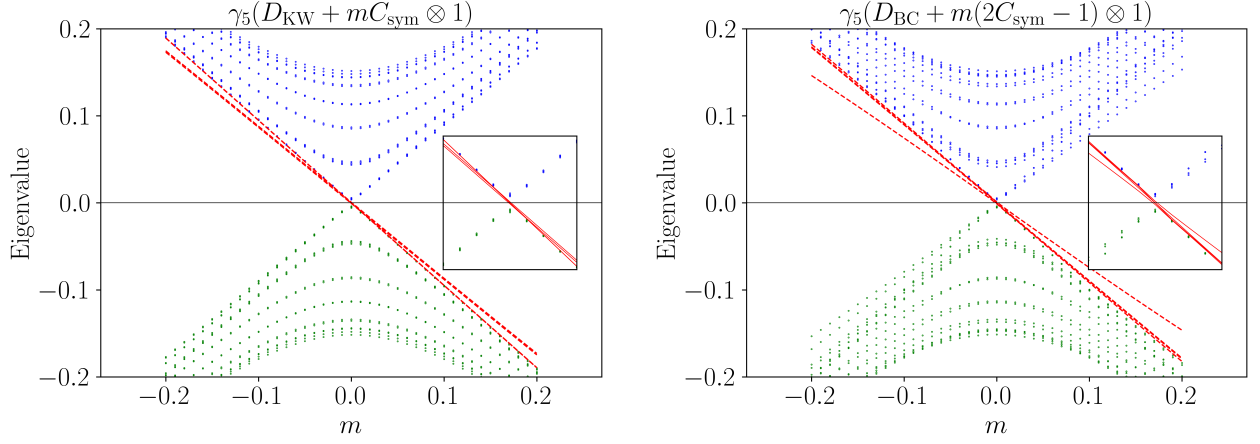


FIG. 11. Spectral flow of the eigenvalues of \mathcal{H} with respect to m for $Q = -1.997$ background $16^3 \times 48$ MILC lattice. In the insets, the x-and y-axis ranges are from -0.04 to 0.04 . Total four nearly overlapping lines (red in color) cross the zero eigenvalue line at $m = 0$. The color coding is intended to guide the eye.

Unsurprisingly, with the MILC lattices too we find $\langle \gamma_5 \rangle \approx 0$ and consequently γ_5 fails to distinguish the chiralities of the low-lying modes. This necessitates the use of modified chirality operator \mathcal{X} defined in Eq. (27). A selection of near-zero eigenvalues, in increasing order, of $H(m=0) \equiv \mathcal{H}(m=0)$ and its chirality determined from the $\langle \mathcal{X} \rangle$ are given in Table V. The corresponding plot is given in Fig. 12.

Eigenvalue of $H_{\text{KW}}(m=0)$	$\langle \psi_i \mathcal{X}_{\text{KW}} \psi_i \rangle$	Eigenvalue of $H_{\text{BC}}(m=0)$	$\langle \psi_i \mathcal{X}_{\text{BC}} \psi_i \rangle$
-4.467×10^{-5}	-9.490×10^{-1}	-4.079×10^{-5}	-9.504×10^{-1}
4.467×10^{-5}	-9.490×10^{-1}	4.079×10^{-5}	-9.504×10^{-1}
-6.052×10^{-4}	-8.762×10^{-1}	-1.011×10^{-3}	-8.738×10^{-1}
6.052×10^{-4}	-8.762×10^{-1}	1.011×10^{-3}	-8.738×10^{-1}
-3.882×10^{-3}	-3.170×10^{-2}	-3.942×10^{-3}	-6.118×10^{-2}
3.882×10^{-3}	-3.170×10^{-2}	3.942×10^{-3}	-6.118×10^{-2}
-4.509×10^{-3}	-1.666×10^{-2}	-4.940×10^{-3}	-1.978×10^{-2}

TABLE V. Eigenvalues and modified chirality \mathcal{X} using eigenvectors of $H(m=0)$ for $Q = -1.997$ background $16^3 \times 48$ MILC lattice.

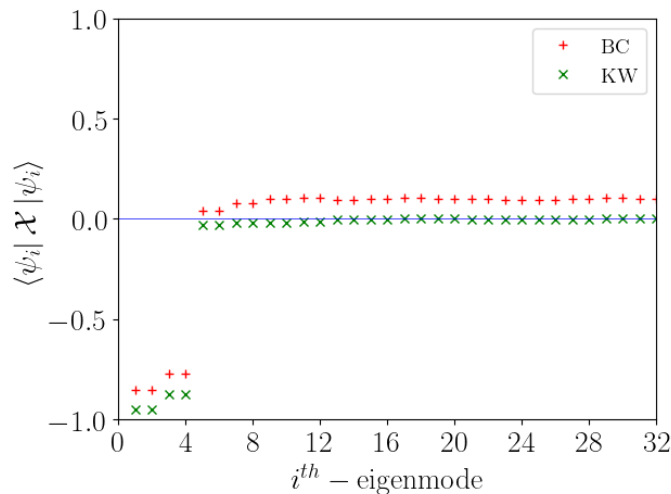


FIG. 12. The modified chirality \mathcal{X} for $Q = -1.997$ background $16^3 \times 48$ MILC lattice. For clarity, $\langle \mathcal{X}_{BC} \rangle$ is shifted by +0.1.

V. SUMMARY AND CONCLUSION

The major advantage of MDF is that they describe two flavors of fermions on a lattice without explicitly breaking the chiral symmetry. This makes MDF a strong candidate for lattice simulations of chiral fermions using an ultralocal action. So far, the chiral properties of MDF, particularly KW and BC fermions, have been studied primarily in two space-time dimensions. A natural next step is to investigate them in four space-time dimensions before considering MDF for realistic QCD calculations. In this work, we have shown that in four space-time dimensions both KW and BC fermions satisfy the Atiyah-Singer index theorem on the lattice in the presence of integer topological charge. The spectral flow of the eigenvalues of the hermitian Dirac operator is used to determine the index on the lattice. We consider two types of gauge backgrounds: the Smit-Vink gauge fields with fixed topological charge and the MILC $N_f = 2 + 1$ asqtad lattices. To improve the signals, the Smit-Vink configurations are appropriately roughened, while the MILC lattices are cooled prior to the measurement of the topological charge and the spectral flow.

The two doublers (or tastes) of MDF with degenerate masses cancel the contributions of opposite chiral states, resulting in a vanishing index despite a non-zero topological charge background. To resolve this, a flavor-dependent mass term, determined by the chiral charges, is introduced. This mass term assigns positive and negative masses to different flavors. The hermitian MDF Dirac operator with the flavor-dependent mass term then yields an index consistent with the index theorem, as observed from the spectral flow of its eigenvalues. The theorem is further verified by measuring the fermionic topological charge. To distinguish the chirality of the zero and non-zero eigenmodes, a corresponding modification of γ_5 is required. The resulting flavor-dependent chirality operator successfully separates the chiralities.

ACKNOWLEDGMENTS

The numerical computations have been performed on the HPC and PARAM Sanganak facilities at IIT Kanpur, funded by DST and IIT Kanpur, as well as on the Proton cluster at NISER, Bhubaneswar. A.K. thanks Stephan Dürr for valuable discussions during LATTICE2024 and subsequent email correspondence, and Taro Kimura for useful email communications. He is especially grateful to Johannes Weber for extensive discussions that ultimately led to the removal of spurious eigenvalues of the hermitian Dirac operator. He also thanks Radhamadhab, Sachin, Aritra, Indrajit, and Akash for insightful discussions on eigenvalues and for fostering a stimulating research environment in the lab at NISER. He acknowledges Diptarko for assistance with Python code for eigenvalue computations, and Abhishek, Manisha, and Dipak at IIT Kanpur for helpful discussions that enhanced his understanding of topology and numerical techniques for eigenvalue calculations.

Appendix A: Some results for background MILC lattice with $Q = 2.995$

Here we present some results for both KW and BC fermions with MILC lattice background gauge field for topological charge $Q = 2.995$. All the calculations are performed on a $16^3 \times 48$ lattice.

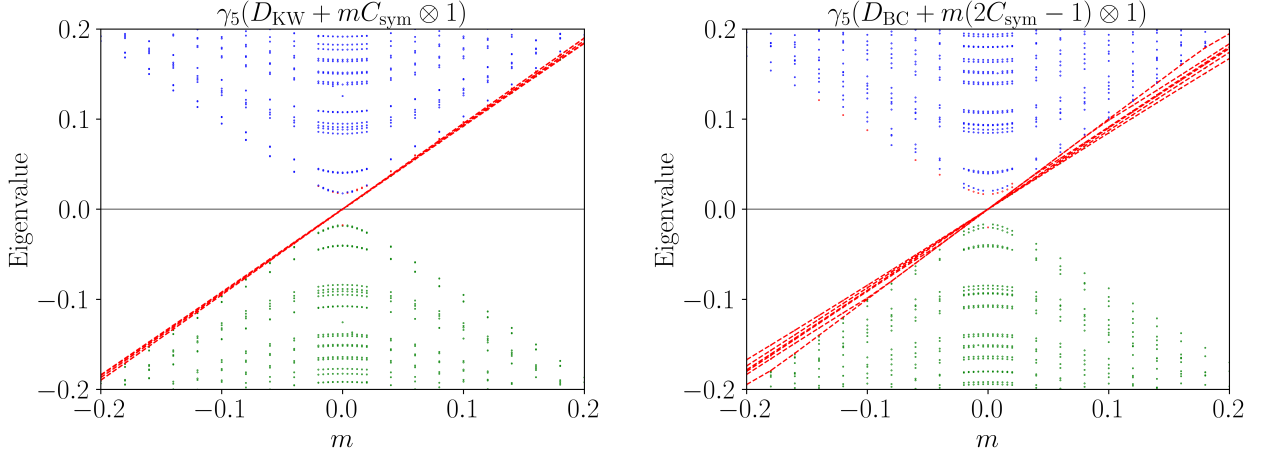


FIG. 13. Spectral flow of the eigenvalues of \mathcal{H} with respect to m for $Q = 2.995$ background $16^3 \times 48$ MILC lattice. Total six nearly overlapping lines (red in color) cross the zero eigenvalue line at $m = 0$. The color coding is intended to guide the eye.

Eigenvalue of $H_{\text{KW}}(m=0)$	$\langle \psi_i \mathcal{X}_{\text{KW}} \psi_i \rangle$	Eigenvalue of $H_{\text{BC}}(m=0)$	$\langle \psi_i \mathcal{X}_{\text{BC}} \psi_i \rangle$
-6.809×10^{-5}	9.442×10^{-1}	-9.210×10^{-5}	9.456×10^{-1}
6.809×10^{-5}	9.442×10^{-1}	9.210×10^{-5}	9.456×10^{-1}
-1.159×10^{-4}	9.427×10^{-1}	-1.136×10^{-4}	9.326×10^{-1}
1.159×10^{-4}	9.427×10^{-1}	1.136×10^{-4}	9.326×10^{-1}
-2.786×10^{-4}	9.263×10^{-1}	-1.766×10^{-4}	9.361×10^{-1}
2.786×10^{-4}	9.263×10^{-1}	1.766×10^{-4}	9.361×10^{-1}
-1.762×10^{-2}	6.264×10^{-3}	-1.654×10^{-2}	1.346×10^{-2}
1.762×10^{-2}	6.264×10^{-3}	1.654×10^{-2}	1.346×10^{-2}
-1.858×10^{-2}	6.886×10^{-3}	-2.021×10^{-2}	-2.183×10^{-5}

TABLE VI. Eigenvalues and modified chirality \mathcal{X} using eigenvectors of $H(m=0)$ for $Q = 2.995$ background $16^3 \times 48$ MILC lattice.

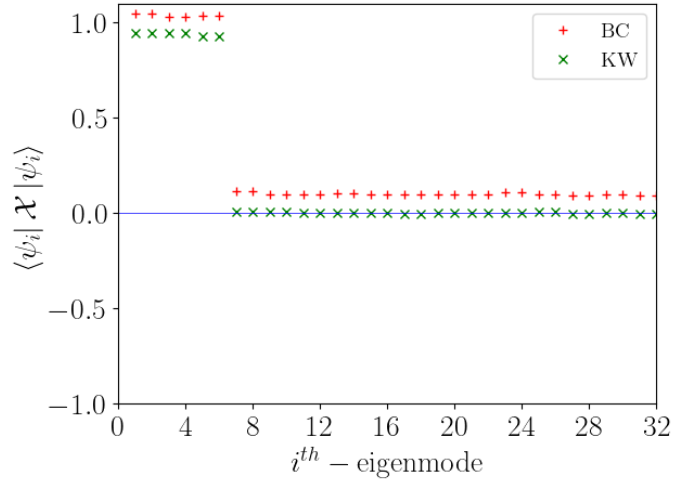


FIG. 14. The modified chirality \mathcal{X} for $Q = 2.995$ background $16^3 \times 48$ MILC lattice. For clarity, $\langle \mathcal{X}_{\text{BC}} \rangle$ is shifted by $+0.1$.

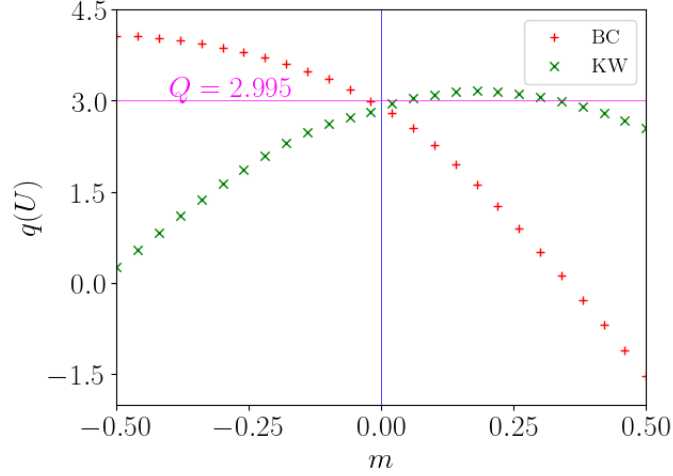


FIG. 15. Variation of fermionic topological charge with m for $Q = 2.995$ background $16^3 \times 48$ MILC lattice.

Appendix B: Eigenvectors of hermitian matrix H from eigenvectors of Dirac operator D and their chiralities

Acting γ_5 on Eq. (6) from left gives

$$\implies \gamma_5 D |\psi_j\rangle = i\lambda_j \gamma_5 |\psi_j\rangle \quad (B1)$$

$$\implies -D \gamma_5 |\psi_j\rangle = i\lambda_j \gamma_5 |\psi_j\rangle \quad \because \{\gamma_5, D\} = 0$$

$$\implies D[\gamma_5 |\psi_j\rangle] = -i\lambda_j [\gamma_5 |\psi_j\rangle]. \quad (B2)$$

Hence, if $|\psi_j\rangle$ is an eigenvector of D with eigenvalue $i\lambda_j$, then $\gamma_5 |\psi_j\rangle$ is also an eigenvector of D with eigenvalue $-i\lambda_j$. It is always possible to obtain a space of complete orthonormal eigenvectors $|\psi_k\rangle$ such that $\langle \psi_k | \psi_j \rangle = \delta_{kj}$ since the normality condition ($[D, D^\dagger] = 0$) holds. Using the normality of D and its γ_5 -hermiticity, one can choose simultaneous eigenvectors $|\psi_j\rangle$ of D and γ_5 in the subspace $\lambda_j = 0$, *i.e.*, $\gamma_5 |\psi_j\rangle = \pm |\psi_j\rangle$ [68]. The proof proceeds as follows. Subtracting Eq. (B2) from Eq. (B1), we obtain

$$\begin{aligned} (\gamma_5 D - D \gamma_5) |\psi_j\rangle &= 2i\lambda_j \gamma_5 |\psi_j\rangle \\ \implies [\gamma_5, D] |\psi_j\rangle = 0 &\iff \lambda_j = 0 \end{aligned} \quad (B3)$$

$$\implies D |\psi_j\rangle = 0 \quad \& \quad \gamma_5 |\psi_j\rangle = \pm |\psi_j\rangle. \quad (B4)$$

Now, combining (B4) and $\{\gamma_5, D\} = 0$ leads to

$$\gamma_5 |\psi_j\rangle = \begin{cases} \pm |\psi_j\rangle & \text{for } \lambda_j = 0 \\ |\psi_k\rangle & \text{for } \lambda_j \neq 0 \text{ with } \lambda_j = -\lambda_k \end{cases}. \quad (B5)$$

Thus, in the space of orthonormal eigenvectors $|\psi_j\rangle$ of D , we have

$$\langle \psi_j | \gamma_5 | \psi_k \rangle = \begin{cases} \pm \delta_{jk} & \text{for } \lambda_j = \lambda_k = 0 \\ 1 & \text{for } \lambda_j = -\lambda_k \neq 0 \\ 0 & \text{for } \lambda_j \lambda_k = 0 \text{ and } \lambda_j \neq \lambda_k \\ 0 & \text{for } \lambda_j \lambda_k \neq 0 \text{ and } \lambda_j \neq -\lambda_k \end{cases}. \quad (B6)$$

For $H(m) = \gamma_5(D + m)$, we compute its eigenvalues μ_j and eigenvectors $|\phi_j\rangle$ in terms of the eigenvalues $\pm i\lambda_j$ and the corresponding eigenvectors $|\psi_j\rangle$ and $\gamma_5 |\psi_j\rangle$ of D .

1. Consider the case with $\lambda_j \neq 0$. Construct $H(m)$ in the subspace spanned by $|\psi_j\rangle$ and $\gamma_5 |\psi_j\rangle$:

$$\begin{aligned} H(m) &= \begin{pmatrix} \langle \psi_j | H | \psi_j \rangle & \langle \psi_j | H | \gamma_5 |\psi_j\rangle \\ [\langle \psi_j | \gamma_5 | H | \psi_j \rangle] & [\langle \psi_j | \gamma_5 | H | \gamma_5 |\psi_j\rangle] \end{pmatrix} \\ &= \begin{pmatrix} 0 & -i\lambda_j + m \\ i\lambda_j + m & 0 \end{pmatrix}. \end{aligned} \quad (B7)$$

Its eigenvalues and eigenvectors are

$$|\phi_j\rangle = \frac{1}{\sqrt{2}} \left[|\psi_j\rangle \pm \frac{i\lambda_j + m}{\sqrt{\lambda_j^2 + m^2}} \gamma_5 |\psi_j\rangle \right] \quad \text{with } \mu_j = \pm\sqrt{\lambda_j^2 + m^2}. \quad (\text{B8})$$

Following Eq. (B6), for $m = 0$, the chiralities vanish, *i.e.*,

$$\langle\phi_j|\gamma_5|\phi_j\rangle = 0. \quad (\text{B9})$$

2. Consider the case with $\lambda_j = 0$:

$$H|\psi_j\rangle = \gamma_5(D + m)|\psi_j\rangle = m\gamma_5|\psi_j\rangle = \pm m|\psi_j\rangle. \quad (\text{B10})$$

Hence, eigenvectors $|\psi_j\rangle$ of D corresponding to zero eigenvalues ($\lambda_j = 0$), are also eigenvectors of $H(m)$ with eigenvalues $\mu_j = \pm m$ depending upon their chiralities.

Suppose there are two zero eigenvectors, $|\psi_{j_1}\rangle = |\phi^+\rangle$ and $|\psi_{j_2}\rangle = |\phi^-\rangle$, with positive and negative chirality, respectively. From these, one may construct two orthonormal zero eigenvectors of D that are not necessarily eigenvectors of γ_5 :

$$\begin{aligned} |\zeta_1\rangle &= a_1 |\phi^+\rangle + b_1 |\phi^-\rangle, & \text{with } |a_1|^2 + |b_1|^2 &= 1, \\ |\zeta_2\rangle &= a_2 |\phi^+\rangle + b_2 |\phi^-\rangle, & \text{with } |a_2|^2 + |b_2|^2 &= 1, \end{aligned}$$

where $\langle\zeta_1|\zeta_2\rangle = 0$. The expectation values of γ_5 are given by:

$$\begin{aligned} \langle\zeta_1|\gamma_5|\zeta_1\rangle &= |a_1|^2 - |b_1|^2, \\ \langle\zeta_2|\gamma_5|\zeta_2\rangle &= |a_2|^2 - |b_2|^2. \end{aligned} \quad (\text{B11})$$

Consequently, $\langle\gamma_5\rangle$ can take any value between -1 and $+1$, unless we impose the condition that the states be simultaneous eigenvectors of D and γ_5 within the zero-mode subspace.

-
- [1] J. Smit and J. C. Vink, Remnants of the Index Theorem on the Lattice, *Nucl. Phys. B* **286**, 485 (1987).
- [2] C. W. Bernard, T. Burch, K. Orginos, D. Toussaint, T. A. DeGrand, C. E. Detar, S. Datta, S. A. Gottlieb, U. M. Heller, and R. Sugar, The QCD spectrum with three quark flavors, *Phys. Rev. D* **64**, 054506 (2001), [arXiv:hep-lat/0104002](#).
- [3] M. Creutz, T. Kimura, and T. Misumi, Index Theorem and Overlap Formalism with Naive and Minimally Doubled Fermions, *JHEP* **12**, 041, [arXiv:1011.0761 \[hep-lat\]](#).
- [4] S. Dürr and J. H. Weber, Topological properties of minimally doubled fermions in two spacetime dimensions, *Phys. Rev. D* **105**, 114511 (2022), [arXiv:2203.15699 \[hep-lat\]](#).
- [5] R. Narayanan and R. L. Singleton, Jr., The Overlap formalism and topological susceptibility on the lattice, *Nucl. Phys. B Proc. Suppl.* **63**, 555 (1998), [arXiv:hep-lat/9709014](#).
- [6] R. G. Edwards, U. M. Heller, and R. Narayanan, A Study of practical implementations of the overlap Dirac operator in four-dimensions, *Nucl. Phys. B* **540**, 457 (1999), [arXiv:hep-lat/9807017](#).
- [7] R. G. Edwards, U. M. Heller, and R. Narayanan, Topological susceptibility and zero mode size in lattice QCD, *Nucl. Phys. B Proc. Suppl.* **73**, 500 (1999), [arXiv:hep-lat/9810019](#).
- [8] R. G. Edwards, U. M. Heller, and R. Narayanan, The overlap Dirac operator: Topology and chiral symmetry breaking, *Chin. J. Phys.* **38**, 594 (2000), [arXiv:hep-lat/0001013](#).
- [9] D. H. Adams, Axial anomaly and topological charge in lattice gauge theory with overlap Dirac operator, *Annals Phys.* **296**, 131 (2002), [arXiv:hep-lat/9812003](#).
- [10] D. B. Kaplan, A Method for simulating chiral fermions on the lattice, *Phys. Lett. B* **288**, 342 (1992), [arXiv:hep-lat/9206013](#).
- [11] Y. Shamir, Chiral fermions from lattice boundaries, *Nucl. Phys. B* **406**, 90 (1993), [arXiv:hep-lat/9303005](#).
- [12] T. Blum, N. H. Christ, C. Cristian, C. Dawson, X. Liao, G. Liu, R. Mawhinney, L. Wu, and Y. Zhestkov, Chirality correlation within Dirac eigenvectors from domain wall fermions, *Phys. Rev. D* **65**, 014504 (2002), [arXiv:hep-lat/0105006](#).
- [13] T. Blum *et al.*, Quenched lattice QCD with domain wall fermions and the chiral limit, *Phys. Rev. D* **69**, 074502 (2004), [arXiv:hep-lat/0007038](#).
- [14] H. Fukaya, S. Aoki, T. W. Chiu, S. Hashimoto, T. Kaneko, J. Noaki, T. Onogi, and N. Yamada (JLQCD, TWQCD), Determination of the chiral condensate from QCD Dirac spectrum on the lattice, *Phys. Rev. D* **83**, 074501 (2011), [arXiv:1012.4052 \[hep-lat\]](#).

- [15] R. C. Brower, H. Neff, and K. Orginos, The Möbius domain wall fermion algorithm, *Comput. Phys. Commun.* **220**, 1 (2017), [arXiv:1206.5214 \[hep-lat\]](#).
- [16] G. Cossu, H. Fukaya, S. Hashimoto, T. Kaneko, and J.-I. Noaki, Stochastic calculation of the Dirac spectrum on the lattice and a determination of chiral condensate in 2+1-flavor QCD, *PTEP* **2016**, 093B06 (2016), [arXiv:1607.01099 \[hep-lat\]](#).
- [17] L. H. Karsten, Lattice Fermions in Euclidean Space-time, *Phys. Lett. B* **104**, 315 (1981).
- [18] F. Wilczek, Lattice Fermions, *Phys. Rev. Lett.* **59**, 2397 (1987).
- [19] M. Creutz, Four-dimensional graphene and chiral fermions, *JHEP* **04**, 017, [arXiv:0712.1201 \[hep-lat\]](#).
- [20] A. Borici, Creutz fermions on an orthogonal lattice, *Phys. Rev. D* **78**, 074504 (2008), [arXiv:0712.4401 \[hep-lat\]](#).
- [21] S. Basak, D. Chakrabarti, and J. Goswami, Mixed action with Borici-Creutz fermions on a staggered sea, *Phys. Rev. D* **96**, 074505 (2017), [arXiv:1707.06402 \[hep-lat\]](#).
- [22] D. A. Godzieba, S. Borsanyi, Z. Fodor, P. Parotto, R. A. Vig, and C. H. Wong, Renormalization of Karsten-Wilczek Quarks on a Staggered Background, *PoS LATTICE2023*, 283 (2024), [arXiv:2401.07799 \[hep-lat\]](#).
- [23] J. H. Weber, S. Capitani, and H. Wittig, Numerical studies of Minimally Doubled Fermions, *PoS LATTICE2013*, 122 (2014), [arXiv:1312.0488 \[hep-lat\]](#).
- [24] J. H. Weber, Correlation functions with Karsten-Wilczek fermions, *PoS LATTICE2014*, 071 (2015), [arXiv:1601.06669 \[hep-lat\]](#).
- [25] J. H. Weber, QCD with Flavored Minimally Doubled Fermions, *PoS LATTICE2016*, 250 (2017), [arXiv:1611.08388 \[hep-lat\]](#).
- [26] S. Dürr and J. H. Weber, Dispersion relation and spectral range of Karsten-Wilczek and Borici-Creutz fermions, *Phys. Rev. D* **102**, 014516 (2020), [Erratum: *Phys.Rev.D* **108**, 059903 (2023)], [arXiv:2003.10803 \[hep-lat\]](#).
- [27] S. Borsányi, S. Capitani, Z. Fodor, D. Godzieba, P. Parotto, R. A. Vig, and C. H. Wong, Taste breaking in the minimally doubled Karsten-Wilczek action and its tree-level improvement, *Phys. Rev. D* **111**, 074510 (2025), [arXiv:2502.07354 \[hep-lat\]](#).
- [28] M. Ammer and S. Durr, Eigenvalue based taste breaking of staggered, Karsten-Wilczek, and Borici-Creutz fermions with stout smearing in the Schwinger model, *Phys. Rev. D* **111**, 014511 (2025), [arXiv:2409.15024 \[hep-lat\]](#).
- [29] S. Durr and S. Capitani, Taste-splittings of staggered, Karsten-Wilczek and Borici-Creutz fermions under gradient flow in 2D, *PoS LATTICE2024*, 460 (2025), [arXiv:2411.18237 \[hep-lat\]](#).
- [30] J. H. Weber, Spin-taste structure of minimally doubled fermions, *PoS LATTICE2023*, 353 (2024), [arXiv:2312.08526 \[hep-lat\]](#); J. H. Weber, Spin-taste representation of minimally doubled fermions from first principles: Karsten-Wilczek fermions, *Phys. Rev. D* **112**, 014509 (2025), [arXiv:2502.16500 \[hep-lat\]](#).
- [31] R. Osmanaj and D. Hyka, Minimally doubled fermions and spontaneous chiral symmetry breaking, *EPJ Web Conf.* **175**, 04002 (2018).
- [32] S. Capitani, M. Creutz, J. Weber, and H. Wittig, Renormalization of minimally doubled fermions, *JHEP* **09**, 027, [arXiv:1006.2009 \[hep-lat\]](#).
- [33] R. A. Vig, S. Borsanyi, Z. Fodor, D. Godzieba, P. Parotto, and C. H. Wong, First dynamical simulations with minimally doubled fermions, *PoS LATTICE2023*, 289 (2024), [arXiv:2401.07651 \[hep-lat\]](#).
- [34] S. Capitani, Reducing the number of counterterms with new minimally doubled actions, *Phys. Rev. D* **89**, 014501 (2014), [arXiv:1307.7497 \[hep-lat\]](#).
- [35] S. Capitani, New actions for minimally doubled fermions and their counterterms, *PoS LATTICE2013*, 121 (2014), [arXiv:1308.4512 \[hep-lat\]](#).
- [36] S. Capitani, J. Weber, and H. Wittig, Minimally doubled fermions at one-loop level, *PoS LAT2009*, 075 (2009), [arXiv:0910.2597 \[hep-lat\]](#).
- [37] S. Capitani, J. Weber, and H. Wittig, Minimally doubled fermions at one loop, *Phys. Lett. B* **681**, 105 (2009), [arXiv:0907.2825 \[hep-lat\]](#).
- [38] S. Capitani, M. Creutz, J. Weber, and H. Wittig, Minimally doubled fermions and their renormalization, *PoS LATTICE2010*, 093 (2010), [arXiv:1010.0110 \[hep-lat\]](#).
- [39] R. Osmanaj and D. Khako, Hypercubic symmetry restoration of Borici - Creutz fermions: costs and effects, *PoS LATTICE2021*, 497 (2022).
- [40] T. Kimura, S. Komatsu, T. Misumi, T. Noumi, S. Torii, and S. Aoki, Revisiting symmetries of lattice fermions via spin-flavor representation, *JHEP* **01**, 048, [arXiv:1111.0402 \[hep-lat\]](#).
- [41] T. Misumi, Phase structure for lattice fermions with flavored chemical potential terms, *JHEP* **08**, 068, [arXiv:1206.0969 \[hep-lat\]](#).
- [42] T. Kimura, T. Misumi, and A. Ohnishi, QCD Phase Diagram with 2-flavor Lattice Fermion Formulations, *PoS LATTICE2012*, 079 (2012), [arXiv:1210.6357 \[hep-lat\]](#).
- [43] T. Misumi, T. Kimura, and A. Ohnishi, QCD phase diagram with 2-flavor lattice fermion formulations, *Phys. Rev. D* **86**, 094505 (2012), [arXiv:1206.1977 \[hep-lat\]](#).
- [44] B. C. Tiburzi, Chiral Lattice Fermions, Minimal Doubling, and the Axial Anomaly, *Phys. Rev. D* **82**, 034511 (2010), [arXiv:1006.0172 \[hep-lat\]](#).
- [45] K. Shukre and S. Basak, Symanzik effective action for Karsten-Wilczek minimally doubled fermions, *Phys. Rev. D* **112**, 114501 (2025), [arXiv:2508.09690 \[hep-lat\]](#).
- [46] M. F. Atiyah and I. M. Singer, The index of elliptic operators on compact manifolds, *Bull. Am. Math. Soc.* **69**, 422 (1969).
- [47] E. V. Shuryak and J. J. M. Verbaarschot, Random matrix theory and spectral sum rules for the Dirac operator in QCD, *Nucl. Phys. A* **560**, 306 (1993), [arXiv:hep-th/9212088](#).
- [48] H. Leutwyler and A. V. Smilga, Spectrum of Dirac operator and role of winding number in QCD, *Phys. Rev. D* **46**, 5607

- (1992).
- [49] D. Chakrabarti, S. Hands, and A. Rago, Topological Aspects of Fermions on a Honeycomb Lattice, *JHEP* **06**, 060, [arXiv:0904.1310 \[hep-lat\]](#).
 - [50] M. Pernici, Chiral invariance and lattice fermions with minimal doubling, *Phys. Lett. B* **346**, 99 (1995), [arXiv:hep-lat/9411012](#).
 - [51] C. Gattringer and I. Hip, On the spectrum of the Wilson-Dirac lattice operator in topologically nontrivial background configurations, *Nucl. Phys. B* **536**, 363 (1998), [arXiv:hep-lat/9712015](#).
 - [52] F. D. R. Bonnet, D. B. Leinweber, A. G. Williams, and J. M. Zanotti, Improved smoothing algorithms for lattice gauge theory, *Phys. Rev. D* **65**, 114510 (2002), [arXiv:hep-lat/0106023](#).
 - [53] A. Kishore, S. Basak, and D. Chakrabarti, Eigenspectra of Minimally Doubled Fermions, *PoS LATTICE2024*, 355 (2025), [arXiv:2501.10336 \[hep-lat\]](#).
 - [54] H. B. Nielsen and M. Ninomiya, No Go Theorem for Regularizing Chiral Fermions, *Phys. Lett. B* **105**, 219 (1981).
 - [55] J. Smit and J. C. Vink, Renormalized Ward-takahashi Relations and Topological Susceptibility With Staggered Fermions, *Nucl. Phys. B* **298**, 557 (1988).
 - [56] S. Itoh, Y. Iwasaki, and T. Yoshie, The U(1) Problem and Topological Excitations on a Lattice, *Phys. Rev. D* **36**, 527 (1987).
 - [57] H. Neuberger, Exactly massless quarks on the lattice, *Phys. Lett. B* **417**, 141 (1998), [arXiv:hep-lat/9707022](#).
 - [58] D. H. Adams, Theoretical foundation for the Index Theorem on the lattice with staggered fermions, *Phys. Rev. Lett.* **104**, 141602 (2010), [arXiv:0912.2850 \[hep-lat\]](#).
 - [59] E. Follana, A. Hart, and C. T. H. Davies (HPQCD, UKQCD), The Index theorem and universality properties of the low-lying eigenvalues of improved staggered quarks, *Phys. Rev. Lett.* **93**, 241601 (2004), [arXiv:hep-lat/0406010](#).
 - [60] E. Follana, A. Hart, C. T. H. Davies, and Q. Mason (HPQCD, UKQCD), The Low-lying Dirac spectrum of staggered quarks, *Phys. Rev. D* **72**, 054501 (2005), [arXiv:hep-lat/0507011](#).
 - [61] V. Azcoiti, G. Di Carlo, E. Follana, and A. Vaquero, Topological Index Theorem on the Lattice through the Spectral Flow of Staggered Fermions, *Phys. Lett. B* **744**, 303 (2015), [arXiv:1410.5733 \[hep-lat\]](#).
 - [62] H. Jeong *et al.* (SWME), Chiral symmetry and taste symmetry from the eigenvalue spectrum of staggered Dirac operators, *Phys. Rev. D* **104**, 014508 (2021), [arXiv:2005.10596 \[hep-lat\]](#).
 - [63] T. Kalkreuter and H. Simma, An Accelerated conjugate gradient algorithm to compute low lying eigenvalues: A Study for the Dirac operator in SU(2) lattice QCD, *Comput. Phys. Commun.* **93**, 33 (1996), [arXiv:hep-lat/9507023](#).
 - [64] C. DeTar *et al.*, The MIMD Lattice Computation (MILC) Collaboration, <https://web.physics.utah.edu/~detar/milc>.
 - [65] B. N. Parlett, *The Symmetric Eigenvalue Problem*, Classics in Applied Mathematics (SIAM, Philadelphia, 1998).
 - [66] I. Hip, T. Lippert, H. Neff, K. Schilling, and W. Schroers, The Consequences of non-normality, *Nucl. Phys. B Proc. Suppl.* **106**, 1004 (2002), [arXiv:hep-lat/0110155](#).
 - [67] J. Smit and J. C. Vink, Topological Charge and Fermions in the Two-dimensional Lattice U(1) Model. 1. Staggered Fermions, *Nucl. Phys. B* **303**, 36 (1988).
 - [68] W. Kerler, Dirac operator normality and chiral properties on the lattice, [arXiv:hep-lat/9905010](#) (1999).